Prioritization criteria of objective index for disaster management by satellite image processing

Mohammad Reza Poursaber*[a], Yasuo Ariki[b] and Mohammad Safi[c]
[a]Ph.D Candidate at Graduate School of System Informatics of Kobe University and Academic Staff of Shahid Beheshti University, [b]Professor at Graduate School of System Informatics at Kobe University and [c]Assistant Professor at Shahid Beheshti University

ABSTRACT

The outputs obtained from satellite image processing generally presents various information based on the interpretation technique, selected objects for object based processing, precision of processing, the number and time of images used for this process. This issue should be managed well during a disaster management process based on satellite images. Very high resolution (VHR) optical satellite data are potential sources to provide detailed information on damage and geological changes for a large area in a short time. In this paper, we studied tsunami triggered area, which was caused on 11 March 2011 by Tohoku earthquake, using VHR data from GeoEye-1satellite images. A set of pre and post-earthquake images were used to perform visual change analysis through comparison of these data. These images include the data of the same area before the disaster in normal condition and after the disaster which caused changes and also some modification imposed to that area. Upon occurrence of a disaster, the images are used to estimate the extent of the damage. Then based on disaster management criteria and the needs for recovery and reconstruction, the priorities for object based classification indexes are defined. In post-disaster management, they are used for reconstruction and sustainable development activities. Finally a classified characteristic definition has been proposed which can be used as sample indexes prioritization criteria for disaster management based on satellite image processing. This prioritization criteria are based on an object based processing technique and can be further developed for other image processing methods.

Keywords: Satellite Image Processing, Object Based Classification, GeoEye-1 Images, Disaster Management

1. INTRODUCTION

An earthquake of magnitude 9.0 occurred off the Pacific coast of Tohoku, Japan, on March 11, 2011, at 14:46:23 Japan Standard Time (5:46:23 UTC). The rupture area, assumed to be approximately 450 km × 200 km, generated a tsunami 130 km off the coast of Miyagi Prefecture, northeast Japan. This tsunami was the third mega earthquake generated tsunami in this decade; the other two were the Sumatra tsunami and the Chile tsunami[1]. Its epicentre was approximately 70 km east of Japan's Oshika Penisula, while its hypocenter was 35 km underwater. With a magnitude of Mw 9.0, this was the strongest earthquake ever to hit Japan and one of the five most powerful earthquakes measured in the world since modern record keeping began in 1900.

Such was the earthquake's force that it moved the island of Honshu – Japan's mainland, or largest island – 2.4 m east, and is also believed to have shifted the earth on its axis by between 10 cm and 25 cm. The earthquake triggered a massive tsunami which reached Japan's east coast in less than one hour. Like the earthquake, the tsunami's severity was unprecedented, both in height and reach. A number of coastal cities were completely inundated. In the northern city of Miyako, the flooding from the tsunami reached a height of 40.5 m. In some of the rivers in Sendai plane, the tsunami impacts could be felt up to 10 km upstream. However, the most heavily impacted areas were in the three prefectures of Miyagi, Fukushima and Iwate, which lay closest to the earthquake's epicenter.

*poursaber,m@me.cs.scitec.kobe-u.ac.jp

Earth Resources and Environmental Remote Sensing/GIS Applications V, edited by Ulrich Michel, Karsten Schulz, Proc. of SPIE Vol. 9245, 92451M · © 2014 SPIE
CCC code: 0277-786X/14/$18 · doi: 10.1117/12.2067253

Japan is considered one of the best disaster-prepared countries in the world. Yet the triple disaster left close to 20,000 people dead or missing (in total 15,854 dead and 3,155 missing as at March 2012, according to official Japanese Government figures). Hundreds of thousands of houses and other buildings were damaged and more than 400,000 people were displaced. With damage estimated at more than USD 210 billion (¥21,000 billion), this event is not only tragic in terms of its human toll; it is the most economically devastating disaster in history. Ishinomaki is a medium-sized municipality located 95 km west of the earthquake's epicentre. Predominantly a fishing centre, it had a population of 162,822 at the time of the event. The first tsunami wave arrived in Ishinomaki at 15:26. The tsunami left the city and its residents completely devastated. As of March 2012, there were 3,280 people confirmed dead and 595 missing. An estimated 6.16 million tons of debris was generated with some 53,742 buildings damaged.

While all of the urban areas along the Tohoku coast were overwhelmed by the amount of tsunami debris, the situation was most grave in the city of Ishinomaki, which suffered the most casualties, the greatest destruction of houses and the highest volume of debris of all the municipalities. The debris management effort in Ishinomaki is being handled jointly by the municipality and the Miyagi prefecture. To the credit of local officials, in just 12 months almost all loose debris from the impacted area has been collected and moved to interim storage locations. The material has been segregated into categories such as wood, automobiles, housing appliances, traditional beds (tatami) and building debris. There is a large storage yard containing fresh timber collected from a protection forest which was overrun by the tsunami. Ishinomaki officials are considering all possible avenues for disaster debris management to overcome the huge challenge posed. The sheer volume of debris remains a significant hurdle for local officials. Spontaneous fires had occurred in some of the mixed waste piles. While passive venting systems have been put in place, fire hazard remains a threat which will become acute in the summer.

An incineration facility, the biggest in Japan (with a processing capacity of 1,500 t/day) consisting of multiple incinerator modules, is being set up and is expected to be operational by August 2012. The municipality has received agreement from the national government to use part of the disaster debris and the incinerator ash for land reclamation within the Ishinomaki port. Once the local paper mill damaged in the earthquake is operating again, it is likely that large quantities of the raw wood will be sent there for use after salt levels in the wood have dropped to acceptable levels.

At the incineration facility visited, there were good health and safety arrangements in place, including fencing, visitor registration, personal protective equipment arrangements for the staff and visitors[2]. For disaster response and relief activities, the actual devastated extent should be indicated as soon as possible. In addition, the recovery and reconstruction activities require determining the structural vulnerabilities in the affected area. To meet this requirement, it is very effective to use remote sensing technology such as image processing or visual inspection of very high spatial resolution (VHR) satellite.[3] The Geoeye-1 satellite images were captured, which include significant information to comprehend the impact of this event. The primary objective of this research is inspecting building damage to identify the extent of affected area and the structural vulnerabilities. In this research, we focus on the coastal districts in Ishinomaki City Miyagi Prefecture, Japan, shown in Fig. 1 and conduct a visual inspection of satellite image for identifying the local vulnerability with particular regard to structural damage. Furthermore, a proportion of the devastated buildings in inundation zone is estimated in the city. Then object-based classification will discuss to the local vulnerabilities in the tsunami affected area.

2. STUDY AREA AND DATA ACQUISITION

The study area is located in Ishinomaki city. The data which used in this study is a very high spatial resolution (VHR) Geoeye-1 satellite imagery data taken from Geoeye-1 sensor on the area in 25 June. 2010 (Before), 19 March. 2011 (During) and 23 May. 2013 (After) the event. The images of Ishinomaki City were obtained 8 months and 15 days before (25 June 2010), 8 days during (19 Mar. 2011) and 26 months after the event. Figure 1 shows the study area and Figure 2.a, b and c show GeoEye-1 satellite images, False color composite (FCC) for the city, before, during and after the event. Ishinomaki is the second biggest city in Miyagi Prefecture, with Sendai being the biggest. Ishinomaki was a fishing town with a population of approximately 160,000 before the earthquake. Following the quake, the number of dead and missing was 4,043.The city has a fishery port as well as an industrial port, both of which were seriously damaged by the tsunami. Ishinomaki, a municipality of Miyagi prefecture, suffered the greatest damage of all the disaster-struck areas in Japan[4]. Base on the reports, the water receded from the areas surrounding the facilities and making access possible on 16 March 2011[5].

Figure 1. Case study site in Ishinomaki, Japan, 2014 Google map

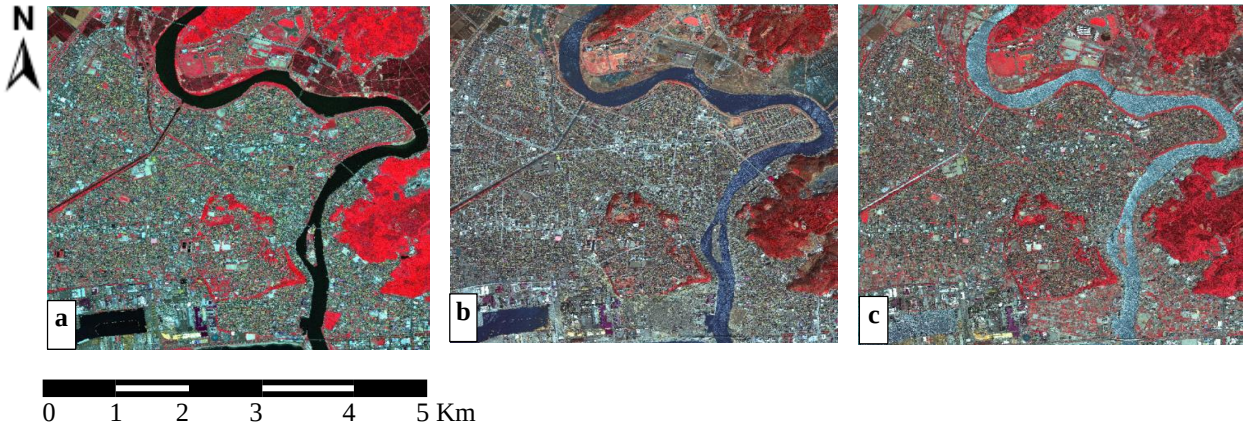

Figure 2. GeoEye-1 Satellite Image, False Color Composite (FCC) of the images, Ishinomaki City
a. Before (25 June. 2010), b. During (19 Mar. 2011) and c. After (23 May. 2013)

3. METHODOLOGY

The methodology in this study includes data processing, using object-based image classification by using a SVM classifier which the defined set of classes can be separated automatically, post classification and accuracy assessment. Finally, the damaged area mapping using the image classification was tried based on land cover classification map and change detection. Figure 3 shows the methodology implemented in this study.

There were four steps in this study. Firstly visual detection of disaster from pre, during and post-event images was performed, preliminarily. Secondly, damage areas were extracted using an object-based method. Then, based on the visual detection result and supervised image classification the accuracies of the automated detection methodology were evaluated, which is mentioned in the next section. Finally by comparing the three images and damage area classified maps it will possible to find statistical change detection and the qualification for the disaster management after the event in the study area.

3.1 Processing Techniques

The processing techniques applied to the images were object-based image classification and change detection statistics in order to compare the results.

3.2 Supervised Image Classification by SVM

In this study, supervised classification algorithms are applied in object-based image classification and Support Vector Machine (SVM) is employed. Recently, particular attention has been dedicated to SVM as a classification method. SVMs have often been found to provide better classification results that those of other widely used pattern recognition methods, such as the maximum likelihood and neural network classifiers. Thus, SVMs are very attractive for the classification of remotely sensed data.

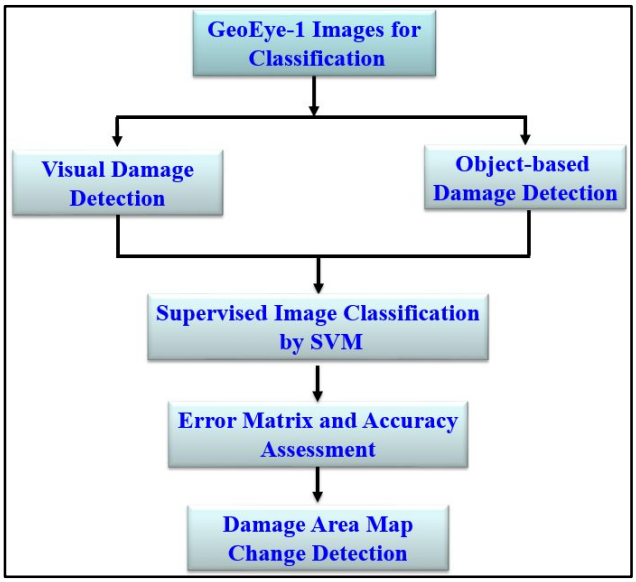

Figure 3. Flowchart of the operations

The SVM approach seeks to find the optimal separating hyper-plane between classes by focusing on the training data that are placed at the boundary of the class descriptors. These training data are called support vectors. Training data other than support vectors are discarded. This way, not only is an optimal hyper plane fitted, but also less training samples are effectively used; thus high classification accuracy is achieved with small training sets. This feature is very advantageous, especially for remote sensing datasets and more specifically for object-based image analysis, where object samples tend to be less in number than in pixel-based approaches (Angelos Tzotsos, 2006)[6].

To summarize, given a set of training data from each class, the objective is to establish the decision boundaries in the feature space which separate data belonging to different classes.

- In the statistical approach, the decision boundaries are determined by the probability distributions of the data belonging to each class, which must either be specified or learned.

- In the discriminant-based approach, the decision boundary is constructed explicitly (i.e., knowledge of the form of the probability distribution is not required):

(1) First a parametric form of the decision boundary (e.g., linear or quadratic) is specified.

(2) The "best" decision boundary of the specified form is found based on the classification of the training patterns[7].

3.3 Object-based image classification

Applying the object-based paradigm to image analysis refers to analyzing the image in object space rather than in pixel space, and objects can be used as the primitives for image classification rather than pixels[8]. Segmentation is the process

of dividing an image into segments that have similar spectral, spatial, and/or texture characteristics. The segments in the image ideally correspond to real-world features. Effective segmentation ensures that the classification results are more accurate[9].

Image segmentation is the primary technique that is used to convert an image into multiple objects. An object has, as compared to a pixel, in addition to spectral values, numerous other attributes, including shape, texture, and morphology that can be used in image analysis. Image segmentation is the process of parting an image into segments by grouping neighboring pixels with similar feature values (brightness, texture, color, etc.). These segments ideally correspond to real-world objects. By suppressing weak edges at different levels, the algorithm can yield multi-scale segmentation results from finer to coarser segmentation[8]. This parameter scale level can ensure that a feature on the image is not divided into too many small segments. Figure 4 shows how pixels group together to form one object through segmentation e.g the roads have become one object.

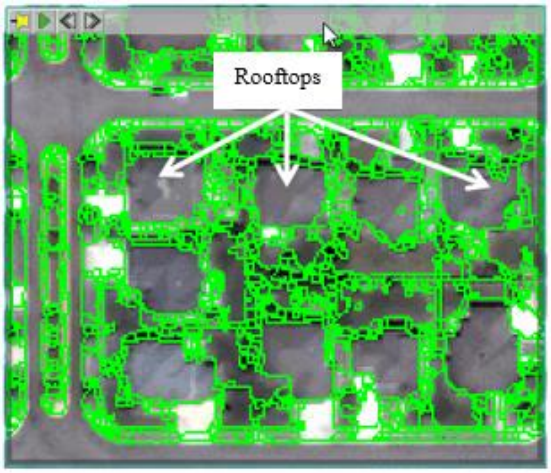

Figure 4. Image segmentation result[9]

3.3.1 Merging Segments

Some features on the image are larger, textured areas such as trees and fields. Merging Segments is employed to aggregate small segments within these areas where over-segmentation may be a problem. In this study we understand if the parameter scale level for merging is 30 and merge level is 85, they will be a useful option for improving the delineation of buildings, roof tops, streets, green field and water boundaries as it is clearly shown in Figure 5.

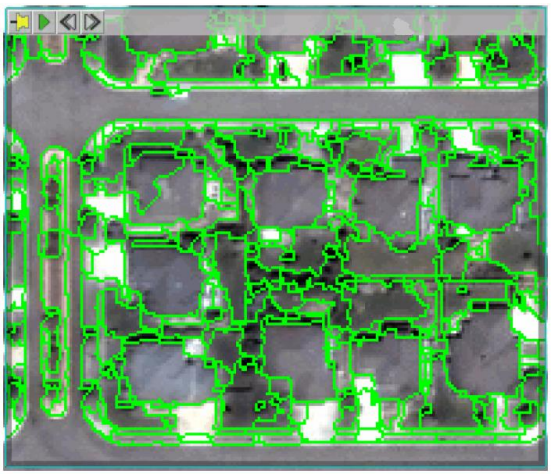

Figure 5. Merging segments[9]

3.3.2 Supervised Classification

The classification procedure starts with an image segmentation based on the single intensity band. After segmentation a supervised classification is performed, using samples for each images in different classes which is shown in Table 1 for supervised classification in Before-event (6 Classes), During (7 Classes) and After-event (8 Classes). Using a SVM classifier the defined set of classes can be separated automatically.

Since in reality most problems are not linearly separable, the data is often transformed into a higher-dimensional space, where a hyper plane can be computed. The drawback of this approach is the high computational load of the transformation. This load can be reduced by using the so called kernel-trick: All inner products are defined as convenient kernel-functions which allow classifying in the higher-dimensional space without having to do any actual computing in it[10].

Table 1. Classes performed in object-based for Before, During and After event by SVM Classifier

Satellite Image	Classification
Before- Event	Roof, Asphalt, Green field, Artificial grass, Water and Soil
During-Event	Survived Roof, Washed away, Debris, Asphalt, Green Field, Water and Soil & Mud
After-Event	Survived Roof, Reconstruction, Debris Classified, Asphalt, Green Field, Water, Soil and Artificial Grass

4. ANALYSIS RESULTS

4.1 Accuracy Assessment

Object-based image analysis approaches have been performed by classifying the remote sensing image. Accuracy assessment of the classification result using the approach has also been done by creating the error matrix. The most common method of accuracy assessment is the Confusion Error Matrix which shows the accuracy of a classification result by comparing with ground truth information. In this study, we used to calculate a confusion matrix using ground truth for regions of interest (ROIs).

In order to compare the accuracy of the classification results created by object-based, the same set of ground truth was used. Then confusion matrixes were produced. Tables 2, 3 and 4 below illustrate user's accuracy, producer's accuracy and overall accuracy for object-based classification method.

Table 2. Accuracy assessment of object-based image classification (Before-Disaster) - Overall Accuracy: 74.5%

Pixels Number	Roof	Asphalt	Green Field	Artificial Grass	Water	Soil & Sand	Total	User. Accuracy (%)
Roof	733514	183432	18626	441	0	2708	938721	78.14
Asphalt	203271	487136	11534	0	143	103	702187	69.37
Green Field	35880	17217	191016	55	236	166	244570	78.10
Artificial Grass	676	1077	0	15985	0	0	17738	90.12
Water	132	0	22	0	9552	0	9706	98.14
Soil & Sand	4590	5565	8499	0	0	7374	26028	28.33
Total	978063	694427	229697	16481	9931	10351	1938950	-
Prod. Accuracy (%)	75.00	70.15	83.16	96.99	96.18	71.24	-	-

Table 3. Accuracy assessment of object-based image classification (During-Disaster) - Overall Accuracy: 70.48 %

Pixels Number	**Survived Roof**	**Washed away**	**Debris**	**Asphalt**	**Green Field**	**Water**	**Soil & Mud**	**Total**	**User. Accuracy (%)**
Survived Roof	172099	31195	9217	7276	1524	16058	8633	246002	69.96
Washed away	45124	821449	123088	5558	1128	4534	108031	1108912	74.08
Debris	3870	22189	136678	246	269	1948	1001	166201	82.53
Asphalt	17606	7159	1017	30036	0	2166	26693	84677	35.47
Green Field	16939	13009	3889	26	38373	1091	1034	74361	51.60
Water	1006	297	19	254	0	19921	0	21497	92.67
Soil & Mud	7081	77963	1738	1778	0	807	147933	237300	62.34
Total	263725	973261	275646	45174	41294	46525	293325	1938950	-
Prod. Accuracy (%)	65.26	84.40	49.58	66.49	92.93	42.82	50.43	-	-

Table 4. Accuracy assessment of object-based image classification (After-Disaster) - Overall Accuracy: 73.24%

Pixels Number	**Survived R.**	**Under Recon.**	**Debris**	**Asphalt**	**Green Field**	**Water**	**Soil**	**Artificial Grass**	**Total**	**User. Accuracy (%)**
Survived Roof	105541	31640	1900	16773	298	1186	8558	381	166277	63.47
Under Recon.	1326	726968	531	17258	17157	0	60866	4	824110	88.21
Debris Classified	2440	1957	18157	338	16	13	0	4	22925	79.20
Asphalt	2641	18553	8	255215	1259	53	32113	0	309842	82.37
Green Field	3748	28766	79	1400	75917	0	3261	34	113205	67.06
Water	0	347	9	0	0	3094	0	67	3517	87.97
Soil	46663	130080	31811	38172	32	4569	222024	1438	474789	46.76
Artificial Grass	2651	3222	241	4749	121	52	0	13249	24285	54.56
Total	165010	941533	52736	333905	94800	8967	326822	15177	1938950	-
Prod. Accuracy (%)	63.96	77.21	34.43	76.43	80.08	34.50	67.93	87.30	-	-

4.2 Result of object-based image classification

The classified image of object-based image classification shows more clear boundaries between objects. Washed away buildings are selected as objects in the image. All the features are illustrated with almost exact shape as it is in the ground truth. The classes of asphalt, green field and water all can be seen without mix classification as can be shown in Figure 6. below.

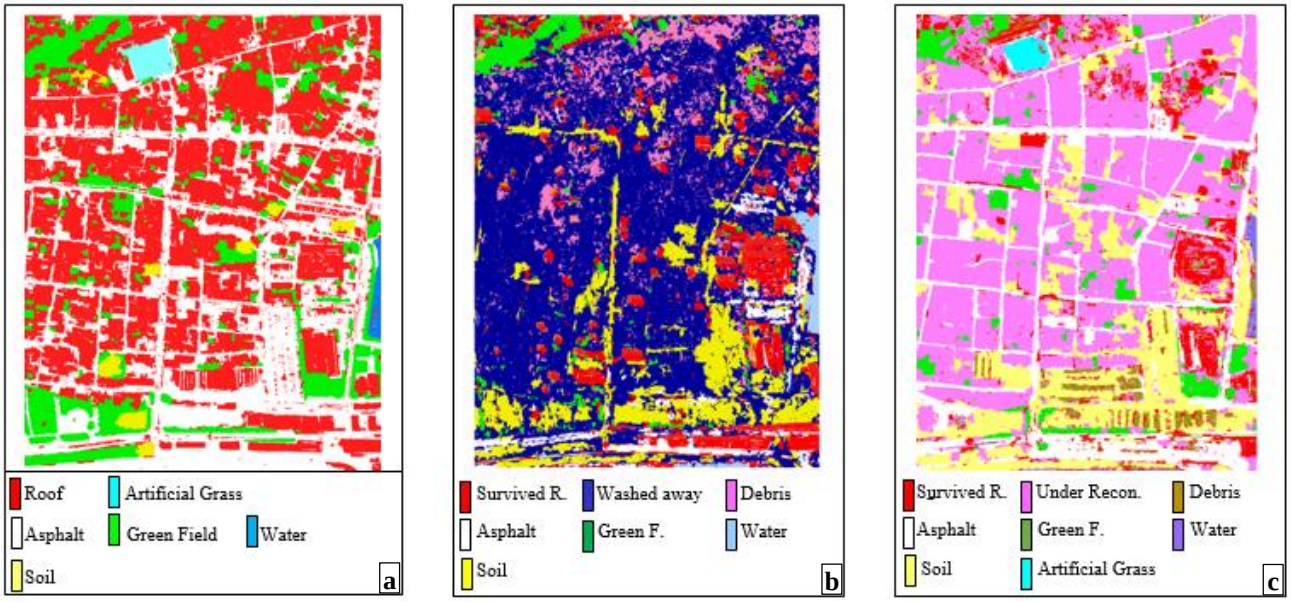

Figure 6. The result of object-based image classification
a. Before, b. During and c. After

5. DISCUSSION

In this study object-based method used in the satellite images. The accuracy depends on the software operator to define classes. When the classes are not clear, the operation is repeated by defining another geometrical shape around the class that was misclassified in the earlier stage of classification. It is shown that in before disaster, F. measure attain more accuracy (77.71%) than during (65.71%) and after (68.09%) disaster. Tables 5 show the accuracy assessment and error results of the object-based image classification analysis for each stage.

Table 5. Errors and accuracies of automated damage detection

Accuracy / Images	Errors (%)		Accuracy (%)		F. measure %
	Commission	Omission	Producer	User	
Before	26.25	17.88	82.12	73.75	77.71
During	33.09	35.44	64.56	66.91	65.71
After	28.80	34.77	65.23	71.20	68.09

Next step is to detect changes. Change detection involves the use of multi temporal data sets to discriminate areas of land cover change between dates of imaging. The types of changes that might be of interest can range from short and term phenomena such as vegetation cover or urban fringe development. Ideally, change detection procedures should involve

data acquired by the same or similar sensor and be reorder using the same spatial resolution, viewing geometry, spectral bands, radiometric resolution and time of day. In this study GeoEye-1 image has a pixel resolution of 0.4 meters. One way to discriminate changes between two dates of images is to employ post classification comparison. In this approach, three dates of imagery are independently classified and registered. Then an algorithm can be employed to determine those pixels with changes in classification between dates.

A variance can be chosen and tested to determine, if it represents a reasonable threshold. The threshold can also be varied interactively in most image analysis system so the analyst can obtain immediate visual feedback on the suitability of a given threshold[11]. The procedures for change detection are based on post classification to compare the Pre-disaster image as initial state image and During disaster as final state image, then to compare During disaster as initial state image and After disaster as final state image which are compared to each other and then it is possible to have change detection statistics based on the pixels number and area (m^2) to find the disaster management progressive in the region. Table 6. and Table 7. show the change detection statistics in both comparative and Fig. 7 and Fig. 8 show the change detection statistics based on m^2.

Table 6. Change detection statistics (Before and During the disaster)

		Before (Initial State)											
		Roof		Asphalt		Green Field		Water		Soil		Artificial Grass	
		Pixels	%	Pixels	%	pixels	%	Pixels	%	Pixels	%	Pixels	%
During (Final State)	Survived Roof	140427	14.96	81314	11.58	20944	8.56	294	3.03	2777	10.67	246	1.39
	Washed away	597933	63.70	369421	52.61	116266	47.54	730	7.52	14717	56.54	9845	55.50
	Debris	101521	10.82	36776	5.24	18926	7.74	16	0.17	1373	5.28	7589	42.78
	Asphalt	18455	1.97	61527	8.76	4534	1.85	0	0.00	161	0.62	0	0.00
	Green Field	25961	2.77	8863	1.26	38457	15.72	0	0.00	1022	3.93	58	0.33
	Water	1814	0.19	7195	1.03	3975	1.63	8513	87.71	0	0.00	0	0.00
	Soil & Mud	52610	5.60	137091	19.52	41468	16.96	153	1.58	5978	22.97	0	0.00
	Class Total	938721	100.00	702187	100.00	244570	100.00	9706	100.00	26028	100.00	17738	100.00
	Class Changes	798294	85.04	640660	91.23	206113	84.28	1193	12.29	20050	77.03	7893	57.22
	Image Difference	-692719	-73.79	-617510	-87.94	-170209	-69.60	11791	121.48	211272	811.71	1091174	836.98

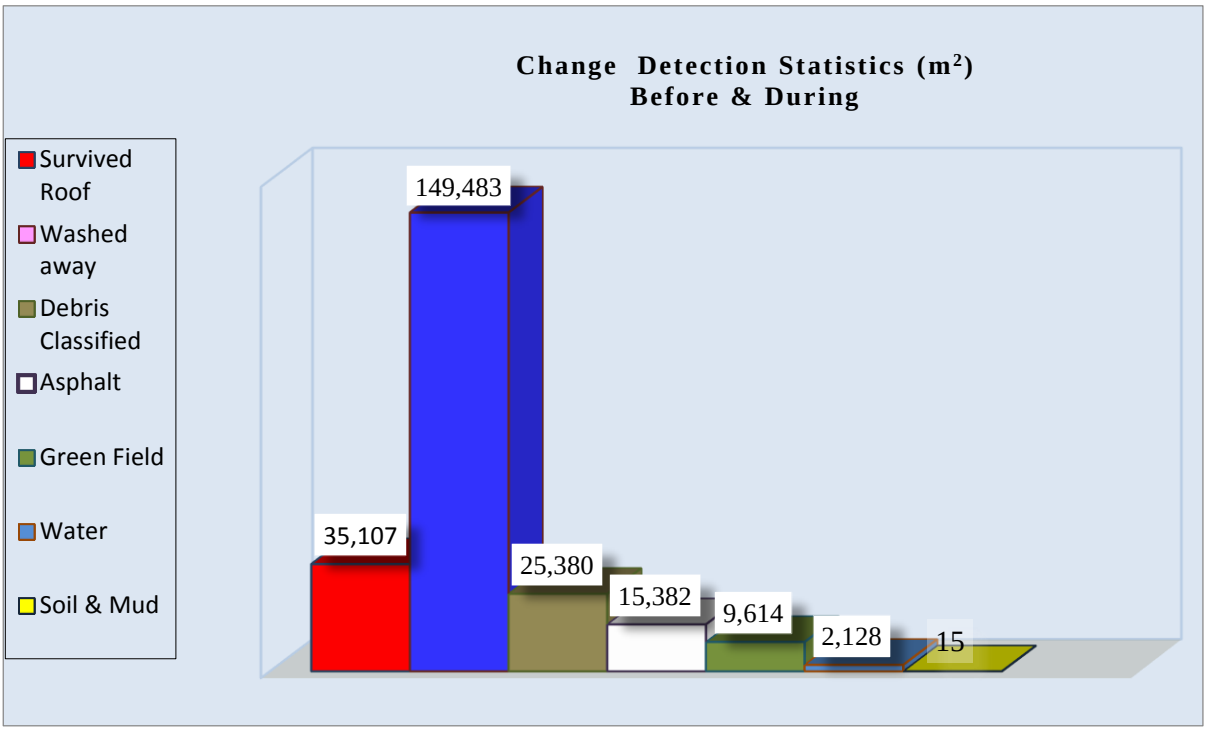

Fig 7. Change detection area (Before and During the disaster)

Table 7. Change detection statistics (During and After the disaster)

After (Final State)	During (Initial State)													
	Survived Roof		Washed away		Debris		Green Field		Water		Asphalt		Soil & Mud	
	Pixel	%	Pixel	%	Pixel	%	Pixel	%	Pixel	%	Pixel	%	Pixel	%
Survived Roof	51985	25.26	55764	50.29	13811	8.31	7734	10.40	1194	5.55	11661	13.77	12942	5.45
Under Reconstruction	50952	26.72	586649	52.90	84848	51.05	18580	24.99	1071	4.98	9883	11.67	51910	21.88
Debris Classified	3108	1.63	10191	0.92	1385	0.83	742	1.00	45	0.21	1298	1.53	5601	2.36
Green Field	7542	3.95	48641	4.39	8056	4.85	34655	46.60	78	0.36	1540	1.82	11486	4.84
Artificial Grass	2249	1.18	11804	1.06	7084	4.26	240	0.32	233	1.08	704	0.83	1378	0.58
Water	281	0.15	231	0.02	9	0.01	0	0.00	2816	13.10	180	0.21	0	0.00
Asphalt	32097	16.83	164521	14.84	16033	9.65	3027	4.07	1719	8.00	38625	45.62	44097	18.58
Soil	42510	22.29	231111	20.84	34975	21.04	9383	12.62	14341	66.71	20786	24.55	109886	46.31
Class Total	190724	100.00	1108912	100.00	166201	100.00	74361	100.00	21497	100.00	84677	100.00	237300	100.00
Class Changes	138739	72.74	522263	47.10	164816	99.17	39706	53.40	18681	86.90	46052	54.39	127414	53.69
Image Difference	-24447	-12.82	-284802	-25.68	-143276	-86.21	38844	52.24	-17980	-83.64	225165	265.91	237489	100.00

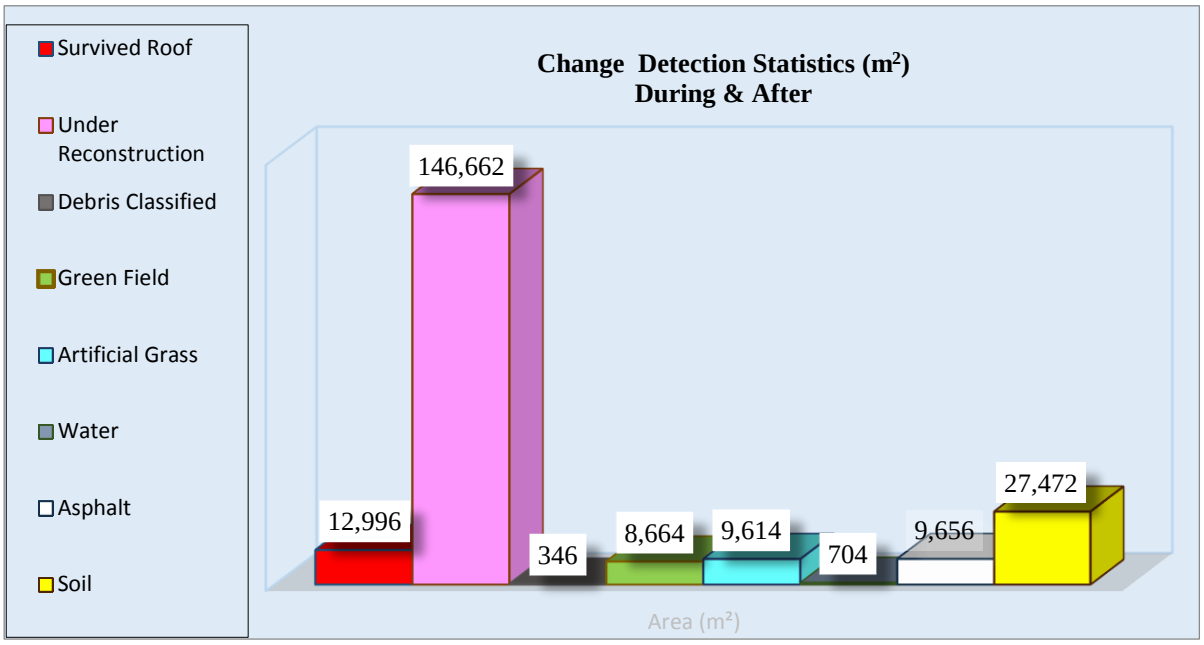

Fig 8. Change detection area (During and After the disaster)

6. CONCLUSION

Based on the classification results obtained from object based method, each selected item give some information which can be used for disaster management. The effectiveness of the classification results depends on the correlation of the results with disaster management objectives and also the accuracy of the results obtained. The main activities for disaster management for waste management are:

To estimate the amount of debris is important for decision makers quickly by using very high resolution satellite imagery. One of the best condition is to keep the amount of transporting of disaster debris and number of times the debris is handled to a minimum. Landfilling and land reclamation are waste management options which have the potential to rapidly reduce the total volume of debris. After the tsunami when the seawater receded, a large volume of soil on the land deposited. To recover, move and dispose of the deposited soil should be based on the physical and chemical properties of the sediments and an analysis of how the residual soil may adversely impact the future land use.

Other main issues are related to emergency actions for life saving and mitigating activities, restoration of facilities such as power, water or gas and other lifelines and reconstruction planning.

However as an example for waste management, the classification item such as debris can be the most suitable factor for management planning. Other related items to this issue are green field and soil for depots, asphalt for transportation routes and survived roofs as a complementary data for debris to identify the concentrated areas for waste and debris transportations. Thus this field of disaster management is necessary to provide the above data with the highest possible accuracy.

The prioritization of the items and criteria can be extracted for each field of disaster management as stated above and by the methods described in the paper. Further study is required to find the correlation of different fields of disaster management to optimize the time and effort for classification.

ACKNOLEDGEMENT

The technical and financial supports by Research Center for Urban Safety and Security (RCUSS) of Kobe University and Shahid Beheshti University are gratefully acknowledged.

REFERENCES

[1] Mori. N, Takahashi. T, Yasuda. T and Yanagisawa. H, "Survey of 2011Tohoku earthquake tsunami inundation", Geophysical Research Letters, Vol. 38, 1-6 (2011).
[2] Gubb. M, "An incinerator under construction in Ishinomaki is due to be the largest in Japan", Managing post-disaster debris, the Japan experience United Nations Environment Programme, 5-50 (2012).
[3] Gokon. H and Koshimura. S, "Mapping of building damage of the 2011 Tohoku earthquake tsunami in Miyagi prefecture", Coastal Engineering Journal, Vol. 54, 1-12 (2012).
[4] Okayama. T, "Disaster Debris Management in Miyagi Prefecture and Ishinomaki City Following the 2011 East Japan Earthquake", ARB Symposium, Hokkaido University, Japan, 1-8 (2013).
[5] Ishii. T, "Medical response to the Great East Japan Earthquake in Ishinomaki City", Vol 2, No 4, 2-4 (2011).
[6] Nghi. D, Mai. L, "An object oriented classification techniques for high resolution satellite imagery", 1-6 (2008).
[7] Burges. C, "A tutorial on support vector machines for pattern recognition", Kluwer Academic Publishers, 637-640 (1998).
[8] Bokhary, Marwa A. M, "Comparison between Pixel Based Classification and Object Base Feature Extraction Approaches for a Very High Resolution Remote Sensed Image", 2-9 (2008).
[9] EXELIS, "Feature Extraction with Example-Based Classification Tutorial", ENVI Tutorial, 2-11 (2012).
[10] Tschanen. K, "Evaluation of Adaptive Image Characteristics for Image Classification", 4-30 (2012).
[11] Tabarroni. A, "Remote Sensing and Image Interpretation Change Detection Analysis: Case Study of Borgo Panigale and Reno Districts", Master II Livello in Sistemi Informativi Geografici, 27-35 (2010).